2022 9th IEEE RAS/EMBS International Conference for Biomedical Robotics and Biomechatronics (BioRob) | 978-1-6654-5849-8/22/$31.00 ©2022 IEEE | DOI: 10.1109/BIOROB52689.2022.9925549

Design and Evaluation of an IMU Sensor-based System for the Rehabilitation of Upper Limb Motor Dysfunction

Bao Tran, Xiaorong Zhang, *IEEE Member*, Amir Modan, and Charmayne M.L. Hughes, *IEEE Member*

***Abstract*— Stroke is one of the most significant non-communicable diseases in the world with approximately 15 million people experiencing a new or recurrent stroke each year. More than half of stroke survivors have some degree of permanent sensorimotor impairment that requires specialized physical rehabilitation. Wearable technologies are a cost-effective means by which to monitor and provide feedback about sensorimotor function across the different phases of stroke recovery, with data-driven insights used to improve clinical decision-making and care experiences. In this paper, we describe the redesign of a single inertial measurement unit (IMU) sensor system (i.e., the T'ena sensor), and evaluate the ability of the sensor to accurately measure movement kinematics during the performance of common post-stroke motor task. Results indicate high to very high agreement and correlation values between the T'ena sensor and the gold-standard motion capture system, regardless of kinematic parameter. In sum, the described T'ena sensor is capable of accurately measuring upper limb movement kinematics, using only a single sensor. The adoption of portable and low-cost devices have the ability to make a substantial impact for the millions of persons who exhibit motor impairments after a stroke.**

I. Introduction

After a stroke, 65% of individuals suffer from upper limb motor impairments [1], such as weakness (hemiparesis), complete paralysis (hemiplegia), proprioceptive deficits, disordered movement organization, decreased range of motion, and impaired force generation. In addition to the substantial limitations in the ability to perform functional tasks, stroke survivors exhibit a reduced capacity for independent living and economic self-sufficiency [2]. Post-stroke arm dysfunction is a key target of stroke rehabilitation protocols, with conventional rehabilitation strategies incorporating repetitive motor or task practice to facilitate neuroplasticity and brain reorganization that drives functional motor recovery [3]. However, this mode of rehabilitation requires frequent in-person interactions with therapists that can last for several months, which invariably places a significant burden on rural and remote communities that struggle with a shortage of specialized health professionals crucial to the delivery of rehabilitative services [4].

*This project was partially supported by the United States National Science Foundation (NSF #2139697 and NSF #1752255).

Bao Tran, Xiaorong Zhang, and Amir Modan are with the School of Engineering at San Francisco State University, San Francisco, CA 94132 USA. (e-mail: btran12@mail.sfsu.edu).

C.M.L. Hughes is with the Health Equity Institute, San Francisco, CA 94132 USA (415-405-2540; e-mail: cmhughes@sfsu.edu).

Fortunately, advances in digital health [5] and wearable sensor technology [6] can alleviate the extant barriers to healthcare access and infrastructure that rural communities face. Inertial measurement units (IMUs) are low-cost portable devices that can precisely and quantitatively measure movement kinematics, which enable clinicians to identify pathological movement, characterize disease state, and track recovery progress [7-11]. For example, [11] utilized a commercially available four-IMU sensor system (Noraxon, USA Inc.) to evaluate post-stroke upper limb kinematics during the finger-to-nose task. Results of that study demonstrated that sub-acute stroke patients' clinical assessment scores (evaluated by the Fugl-Meyer Assessment of Upper Extremity [uFMA]) were highly correlated with mean velocity (r = 0.85), peak velocity (r = 0.81), and moderately the number of movement units (r = -0.65). While the results of that study were promising, the determination of upper extremity kinematic information required multiple sensors and custom written software scripts. Thus, while there are many benefits to using currently available commercial IMU systems, their costs (associated in large part due to the necessity of multiple IMUs) and technical knowledge requirements limit their application to rural communities and decentralized environments (i.e., community centers or patient's home).

Our research group have capitalized on developments in IMU hardware technology and signal processing techniques to develop a low-cost rehabilitation system that uses a single IMU and advanced signal-processing algorithms to record limb movements and derive kinematic metrics that are meaningful to both clinicians and patients [7-8]. The validity of the sensor was recently compared to a gold standard optoelectronic motion capture system [8], with results indicating strong positive correlations and agreement with the gold standard reference system (i.e., optoelectric Vicon motion capture system), regardless of task or kinematic parameter. The sensitivity of the sensor was then tested in patients with acquired brain injury (i.e., stroke, traumatic brain injury) [8], with results demonstrating that the sensor could accurately discriminate between different arm impairment level. Specifically, uFMA scores were significantly correlated with movement time, movement smoothness, mean velocity, and peak velocity.

While the sensor system proved to be a useful tool in the evaluation of sensorimotor dysfunction, the system consisted of cumbersome breakout modules and a portable battery bank that yielded a total volume of 242,748 mm^3 and weight of 450 g (Fig 1A). As such, while limb kinematics could be accurately measured using the sensor, substantial changes needed to be made to improve the weight and robustness of the system before initiating clinical trials in decentralized locations. As such, the aim of the present study was to redesign the system into a single printed circuit board (PCB) and lithium-ion (li-ion) battery. In doing so, a more lightweight and robust commercial version of the sensor (hereafter referred to as the T'ena sensor) can be deployed to decentralized environments, such as community centers or patients' homes.

To this end, participants performed an object manipulation task taken from the Action Research Arm Test (ARAT) [13], while data was simultaneously collected by the T'ena sensor and the Vicon motion capture system. Results of this study will provide a better understanding of the validity and reliability of a single IMU-based sensor system to accurately measuring movement kinematics.

II. METHODS

A. Hardware and Firmware Design of the T'ena Sensor

1) Original Design

The original IMU sensor prototype (Fig. 1A) was comprised of a Tiva C Series TM4C123G microcontroller LaunchPad, a GY-91 MPU-9250 sensor breakout, an HC-05 Bluetooth breakout, and a portable USB power bank. The three breakout boards were encased in a 3D printed polylactic acid (PLA) filament enclosure (83H x 59W x 39D mm) that had a build thickness of 0.25 mm. The sensor was powered by a 2600 mAh USB portable battery (29H x 21W x 85D mm) that was affixed to the top of the enclosure. For the firmware design, raw accelerometer and gyroscope data collected from the GY-91 sensor were read by the microcontroller using an Inter-Integrated Circuit (I^2C) interface. Data was then transmitted to the HC-05 Bluetooth module via Universal Asynchronous Receiver-Transmitter (UART) interface whenever a new data sample was collected. More details about the original sensor design can be found in [7].

2) Design of the T'ena Sensor

The redesigned T'ena sensor system (Fig. 1B) consists of three main components: an ESP32-WROOM32D microcontroller module (Espressif), an ICM20689 IMU sensor (Invensense), and a 400 mAh li-ion battery (Sparkfun). The ESP32-WROOM32D module was chosen for its low cost (single unit cost of $6.825), small size, and the integration of an on-board Bluetooth module. The ICM20689 IMU sensor was selected because of its low cost (single unit cost of $6.09) and similarity to the original MPU-9250 IMU sensor, which is now an end-of-life product. The custom PCB was designed to minimize space and reduce connection fragility, which was an issue with the original sensor due to the use of separate breakout boards. A USB-C connector was integrated into the system and custom circuits were developed to charge, program, and monitor the sensor. Finally, an easy-to-use touch-on-hold-off push button circuit was integrated into the PCB to power the system. The sensor enclosure was designed and manufactured using stereolithographic (SLA) 3D printing. In contrast to PLA 3D printing, SLA uses a laser to cure liquid resin into hardened plastic, and has build lines with a thickness of 0.05 mm. As such, SLA resin parts have five times the layer resolution of acrylonitrile butadiene styrene (ABS) and PLA plastic parts, thereby providing crisper and higher-resolution detail.

In sum, the redesigned sensor system weighed 60 g with a total size of 50H x 70W x 20D mm (total volume of 70,000 mm^3). Thus, the weight of the sensor was reduced by 390 g and the total size by 172,748 mm^3. The firmware of the sensor was also improved by replacing the I^2C-based data collection module with a new module that integrates the Serial Peripheral Interface (SPI) and a First-In-First-Out (FIFO) buffer to achieve higher efficiency and timing precision with processing and transmission of bulk measurements.

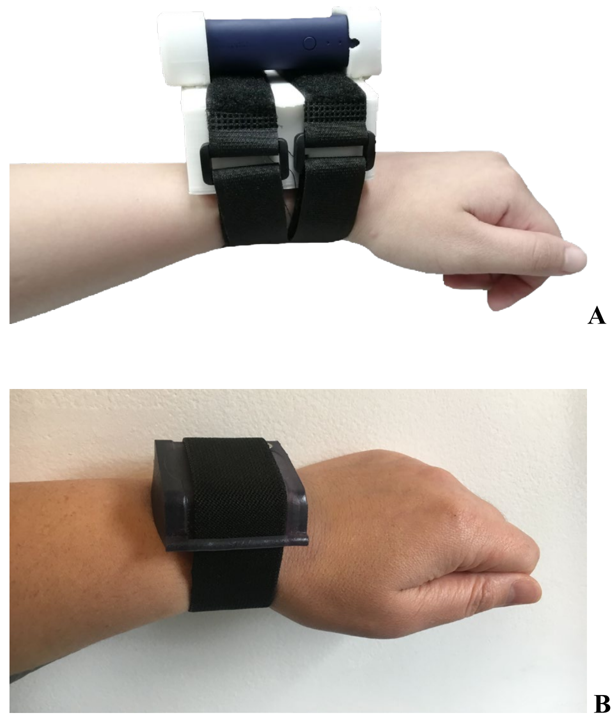

Fig. 1. Original sensor (A: top) and redesigned T'ena sensor (B: bottom) placed on a participant's wrist.

B. Participants

Ten participants from the San Francisco State University campus (mean age = 38.2, SD = 14.9) participated in the present study. Based on administration of the Revised Edinburgh Handedness Inventory [13], all participants were right handed (mean = 93.61, SD = 6.73). The study was approved by the San Francisco State University Institutional Review Board committee.

C. Tested Systems

Initial calibration of the IMU occurred at the start of each data collection session, and consisted of placing the sensor on a flat table until 1,000 data points were captured. During each trial, the raw data were sent from the IMU to the microcontroller via the SPI communication protocol, and then to a custom application on a personal computer via classic Bluetooth which saved the incoming data stream in a CSV file for later off-line processing.

Criterion reference kinematic data was collected using an eight camera Vicon motion capture system (Bonita 10, VICON Motion Systems), with a temporal and spatial resolution of 100 Hz and 1 mm, respectively. One 9.5 mm reflective markers was attached to the top of the T'ena sensor and was used to calculate movement kinematics during task performance.

C. Procedure

After completing the written informed consent forms, the participant sat upright in a chair with the sensor placed on the participant's dominant hand. The validity of the T'ena sensor to capture movement kinematics was evaluated through the performance of a functional task commonly used to evaluate post-stroke upper limb function. The Block Task is one of the functional activities from the grasp subtest of the Action Research Arm Test (ARAT) [12]. In this task, the participant started each trial with their hand on the table in a pronated palm down orientation. Upon the verbal "go" signal, the participant grasped a 5 cm^3 block from the table, placed it on the a 37 cm high shelf placed 25 cm away from the front edge of the table, and then bought their hand back to rest on the starting position. Instructions emphasized that the participant was to perform the task at a comfortable speed, and to grasp the object in such a way that it would not slip during the fingers during the object transportation.

D. Data Processing

For each individual trial, the 3D coordinates of the Vicon marker were reconstructed and labeled, and then exported in CSV format. Using a custom written MATLAB (The MathWorks®, Version R2021a) script, the 3D position data of each axis was transformed into movement velocity using a first-order central difference technique, with the individual vector velocities summed to derive resultant velocity.

The raw gyroscope and accelerometer values obtained from the T'ena sensor were offline processed by a custom program written in MATLAB (The MathWorks, Version R2021a). While more details can be found in [8], the data sets were trimmed based on a stationary detection threshold to exclude stationary sections at the beginning and end of the recorded gesture. A Madgwick Attitude Heading Reference System (AHRS) filter was used to compute the current IMU orientation and transform the data from the local sensor frame to the global earth frame. Additionally, 1 g was subtracted from the z-axis acceleration to account for gravitational acceleration effects. Subsequently, the integral of the acceleration signal was calculated to derive velocity separately for the three axes. Resultant velocity was then calculated by summing the individual vector velocities.

For each Vicon and T'ena sensor trial, data analysis was restricted to the time period between when the hand left the starting position (movement onset) to the time period when the hand returned to the starting position (movement offset). Based on prior literature [7-8], as well as more recent pilot testing, it was expected that the resultant velocity profile would exhibit three peaks for this particular functional task. As such, movement onset and offset were determined using

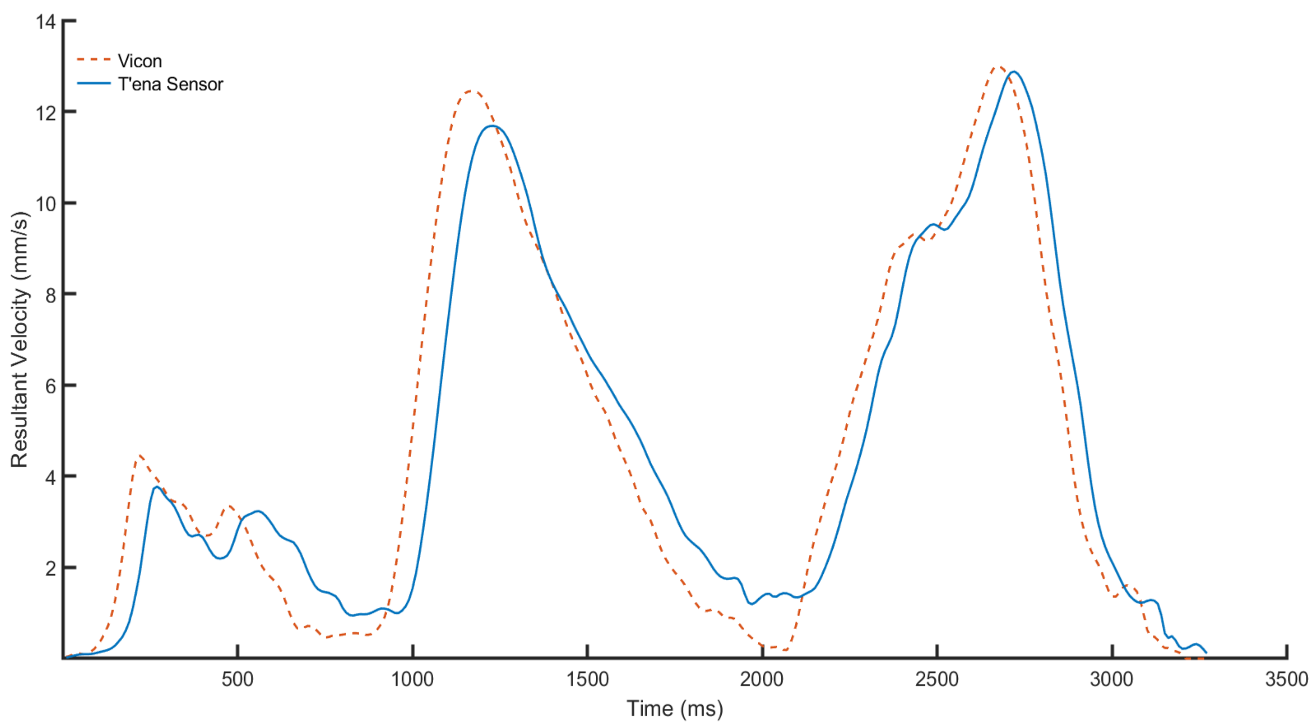

Fig. 2. Representative resultant velocity trajectory for the T'ena sensor (solid blue lines) and the Vicon motion capture system (dashed orange lines).

kinematic criterion. Specifically, movement onset was determined as the instant when resultant velocity exceeded 1.5% of the first velocity peak. Movement offset was determined as the moment when the velocity trace dropped, and remained, below 1.5% of the last peak.

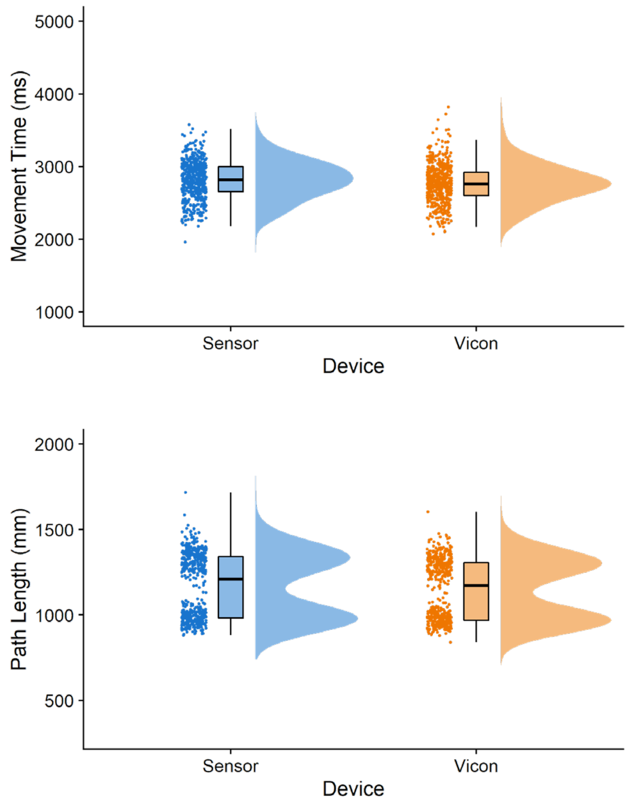

Fig. 3. Raincloud plots showing the data distribution, and five summary statistics for the T'ena sensor (dark grey) and the Vicon motion capture system (light grey) for the movement time (top panel) and path length metrics (bottom panel).

E. Statistical Analysis

Four kinematic variables were derived based on their sensitivity to detect differences in motor dysfunction and use in clinical settings [14]: Total movement time (ms), Path Length (mm), Peak Velocity of the Placing Phase (mm/s), and Peak Velocity of the Return Phase (mm/s). Total movement time was defined as the time period from movement onset to movement offset. Path Length was defined the total displacement of the hand from the beginning to the end of the movement. The Block task can be divided into a placing phase and a return phase. The placing phase was defined as the time period between when the block was lifted from the table to the time the block contacted the shelf top. The return phase was defined as the time period between when the object contacted the shelf top to when the hand was placed on the back on the table. For these two phases, peak velocity was calculated by determining the maximal resultant speed reached in the given phase.

For the aforementioned variables, Pearson product moment correlation coefficients (*r*) were calculated to quantify the degree to which the T'ena sensor and the gold standard Vicon motion capture system were related. Additionally, intra class correlation coefficients (ICC 2,1) were used to evaluate inter-sensor reliability, using the absolute agreement definition between the redesigned sensor and the gold standard motion capture system.

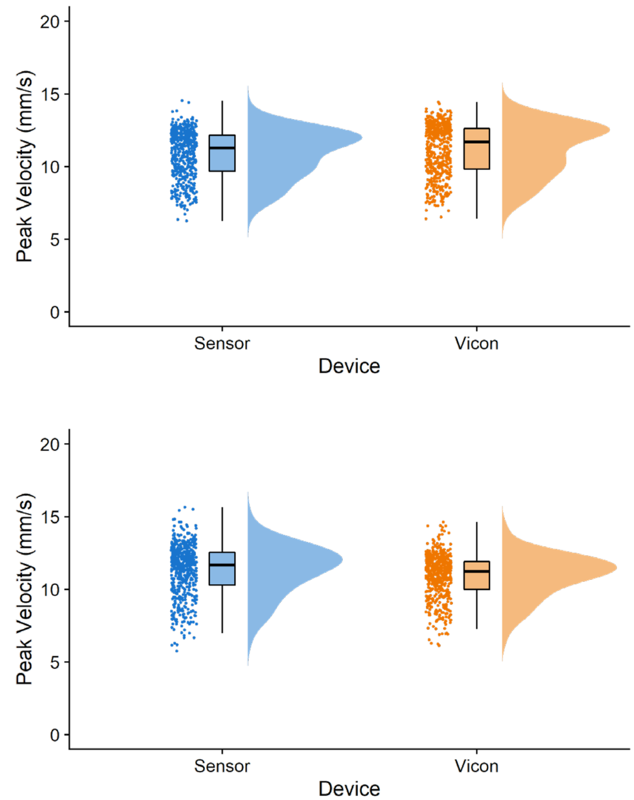

Fig. 4. Raincloud plots showing the data distribution, and five summary statistics for the T'ena sensor (dark grey) and the Vicon motion capture system (light grey) for the peak velocity of the placing phase (top panel) and return phase (bottom panel).

III. RESULTS

Overall, 596 trials where obtained with both the T'ena sensor and a Vicon motion capture system. As can be seen in Fig. 2, the T'ena sensor produced resultant velocity trajectories representative of the Block Task [7-8], with kinematics that were similar to that captured by the gold-standard Vicon motion capture system. Raincloud plots that depict the data distribution and summary statistics (i.e., median, first quartile, third quartile, minimum, and maximum) are shown in Fig 3 (movement time, path length) and Fig 4 (peak velocity of the placing phase, peak velocity of the return phase). In general, the data was normally distributed for the movement time and return phase peak velocity, whereas peak velocity of the placing phase, was positively skewed, and path length exhibited a bimodal distribution. Despite the differences due to kinematic parameter, the shape of the distribution (as well as the five summary statistics values) were similar for both the T'ena sensor and Vicon system.

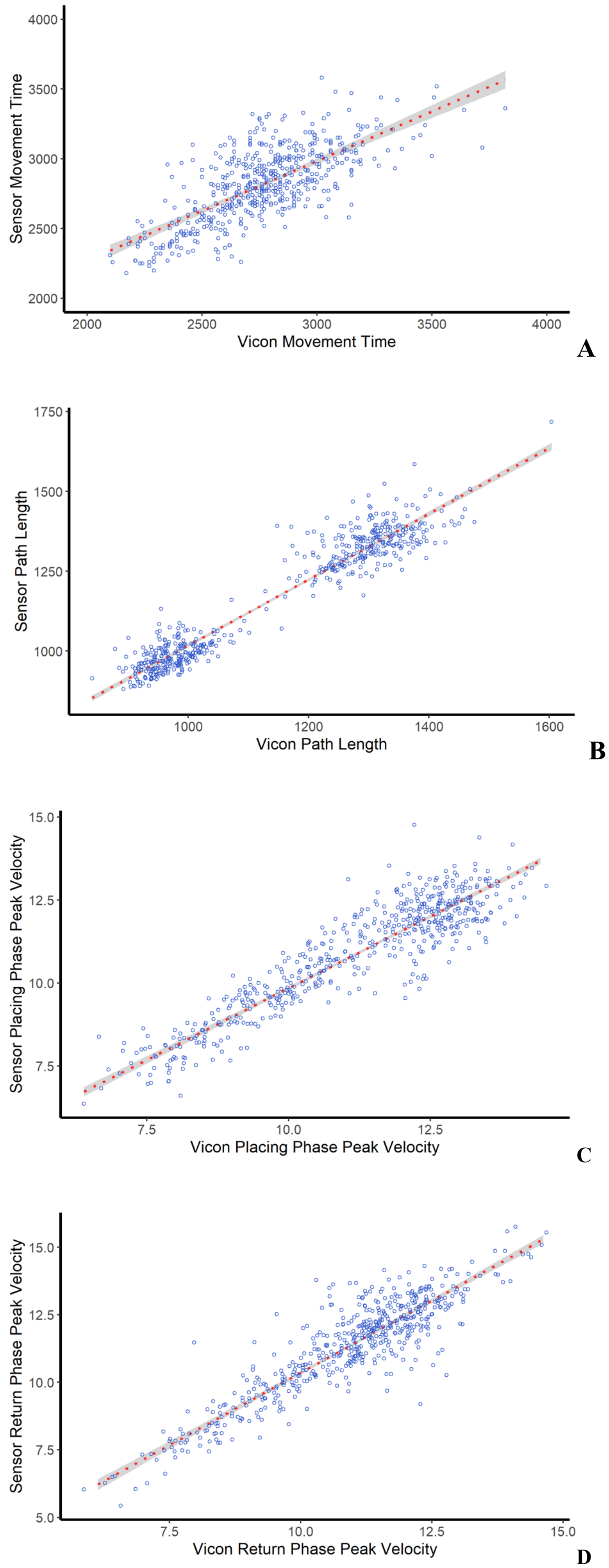

Fig. 5. Correlation plots between the T'ena sensor and Vicon. A) Movement time, B) Path length, C) Peak velocity of the placing phase, and D) Peak velocity of the return phase.

Examining the relationship and absolute agreement between the sensors, it was clear that there was a very high level of agreement for all metrics (Fig 5). Pearson product moment correlation values were strong/high for the movement time variable (r = 0.720), and very strong/very high for path length r = 0.962, peak velocity of the placing phase (r = 0.939), and peak velocity of the return phase (r = 0.917), all p's < 0.05. Intra class correlation coefficients showed a similar pattern of results, with the level of absolute agreement between the two systems classified as strong for the movement time metric (ICC = 0.706), and very strong for the path length (ICC = 0.952), peak velocity of the placing phase (ICC = 0.920), and peak velocity of the return phase (ICC = 0.878).

IV. DISCUSSION

Conventional physical therapy is a time and labor-intensive process that is plagued by low patient engagement, satisfaction, and adherence. Current technology-based solutions involve optoelectric motion capture systems that record 3D position of reflective markers and actuated robotic devices that generate driving forces to help the patient move through space [15-16]. Despite their high accuracy, many of these systems have not been commercially successful because of their high cost, safety issues, and bulkiness that limit their application to decentralized environments (i.e., community centers or patient's home). As such, the aim of the present study was to determine the ability of the T'ena IMU sensor-based system to reliably and accurately assess movement quality and efficiency in physically and neurologically healthy adults.

Statistical analysis indicated high to very high correlations (r range = 0.720 – 0.962) and absolute agreement values (ICC range = 0.706 – 0.952) between the T'ena sensor and reference system, regardless of kinematic metric. Of the four measured kinematic metrics, correlations and absolute agreement values were the lowest for the movement time metric. This is most likely due to the fact that the IMU is less sensitive to the very low acceleration movements that occur at the start and end of the movement. To correct for this issue, future work will involve exploring whether parameter tuning of the stationary detection threshold and/or AHRS filter algorithm can improve the accuracy of the T'ena sensor to detect movement onset and offset. Additionally, we will explore whether deep learning algorithms (e.g., convolutional neural networks) [17] are better able to improve the accuracy of the T'ena sensor by learning the non-dimensional relationship from the high-dimensional data collected by the T'ena sensor and a reference system.

Some of the limitations of the study include the evaluation of a single post-stroke upper limb ADL, and measuring performance in only neurologically healthy individuals. The Block Task was selected because it is a commonly used functional activity from the Action Research Arm Test (ARAT) [12], and was used in our prior work [7-8]. As such, we were able to compare the qualitatively compare the performance of the current T'ena sensor to data collected from neurologically healthy individuals [7] and acquired brain injured individuals [8] using the original version of the sensor. That said, in future studies, we will determine the ability of the T'ena sensor to measure a variety of ADL tasks associated with motor impairment and disability scales, such as the Motor Assessment Scale (MAS), the Melbourne Assessment of Unilateral Upper Limb Function, and the Fugl-Meyer Upper Extremity Motor Assessment [uFMA]). In addition, while the current iteration of the sensor was not tested in post-stroke patients, the original iteration was tested in Ethiopian acquired brain injured patients (e.g., stroke, traumatic brain injury) [8]. In that study, the sensor was found to be sensitive to differences in performance-based upper limb impairment. Thus, future experimental work will focus on measuring motor performance in a heterogeneous sample of post-stroke individuals, with sensor metrics compared with values obtained from clinical scales. This work will enable us to determine the tasks (as well as the level of motor impairment), that the T'ena sensor is capable of accurately measuring.

From a technical and commercialization perspective, performance metrics (e.g., processing delay, communication latency, data loss rate, memory and power consumption) will be measured, after which extensive analysis will be done to evaluate relations and trade-offs between these performance metrics in order to identify optimal settings for the system. Concurrently, the T'ena sensor will be integrated into the T'ena rehabilitation mobile application [18], after which the ability of the system to support recovery for individuals with stroke in their home environment will be examined.

Despite these limitations, the results of the study are promising and highlight the potential of the redesigned T'ena sensor for decentralized rehabilitation of stroke and other neurological (e.g., Huntington's disease, Traumatic Brain Injury) and physical impairments (e.g., work-related musculoskeletal injuries). The research described in this paper is innovative because it proposes a new home-based approach to physical and neurological rehabilitation management, which up until now has been conducted in specialized clinics. The long-term goal of this work is to leverage mobile and wearable technologies to address the primary reasons why patients do not remain compliant with their plan of care – access and convenience. By facilitating the successful establishment of technology-enabled home-based rehabilitation of persons with motor impairments, the T'ena system could lead to a paradigm shift in the way that neurological disorders and physical injuries are managed. From a broader perspective, context-appropriate low-cost technologies can lead to improvements in clinical practice and access to care in medically underserved areas (e.g., health professional shortage areas [HPSAs] and medically underserved areas [MUAs]) or during situations where in-person medical care is contraindicated (e.g., the COVID-19 pandemic).

REFERENCES

[1] A. S. Go *et al*., "Heart disease and stroke statistics—2014 update: a report from the American Heart Association", *Circulation*, vol. 129, no. 3, Dec. 2013, doi: 10.1161/01.cir.0000441139.02102.80.

[2] B. Bates *et al.*, "Veterans affairs/department of defense clinical practice guideline for the management of adult stroke rehabilitation care executive summary", *Stroke*, vol. 36, no. 9, pp. 2049–2056, Sep. 2005, doi: 10.1161/01.STR.0000180432.73724.AD.

[3] L. Carey *et al*., "Finding the intersection of neuroplasticity, stroke recovery, and learning: scope and contributions to stroke rehabilitation". *Neural Plast*, 2019.

[4] C. O. B. Cherry *et al*., "Expanding stroke telerehabilitation services to rural veterans: a qualitative study on patient experiences using the robotic stroke therapy delivery and monitoring system program", *Disabil Rehabilitation Assist*, vol. 12, no. 1, pp. 21-27, 2015, doi: 10.3109/17483107.2015.1061613.

[5] A. Verma, A. Towfighi, A. Brown, A. Abhat, A. Casillas, A, "Moving towards equity with digital health innovations for stroke care", *Stroke*, vol. 29, no. 2, pp. 689-697, 2022.

[6] A. Alamäki *et al*., "Wearable technology supported home rehabilitation services in rural areas: emphasis on monitoring structures and activities of functional capacity". Handbook. Wearable Technology Supported Home Rehabilitation Services in Rural Areas:– Emphasis on Monitoring Structures and Activities of Functional Capacity Handbook., pp. 1-56, 2019.

[7] C. M. L. Hughes *et al*., "Development of a post-stroke upper limb rehabilitation wearable sensor for use in sub-Saharan Africa", *Front Bioeng Biotech*, vol. 7, Nov. 2019, doi: 10.3389/fbioe.2019.00322.

[8] C. M. L. Hughes *et al*., "Quantitative assessment of upper limb motor function in Ethiopian acquired brain injured patients using a low-cost wearable sensor", *Front Neurol*, vol. 10, Dec. 2019, doi: 10.3389/fneur.2019.01323.

[9] S. Patel et al., "A novel approach to monitor rehabilitation outcomes in stroke survivors using wearable technology". Proc IEEE, vol. 98, no. 3, pp. 450–461, 2010.

[10] A. R. Parnandi, E. Wade, M. Mataric, "Motor function assessment using wearable inertial sensors". Conf Proc IEEE Eng Med Biol Soc, pp. 86-89, 2010.

[11] Z. J. Chen, H. Chang, M. H. Gu, J. Xu, X. L. Huang, "Kinematic evaluation via inertial measurement unit associated with upper extremity motor function in subacute stroke: A cross-sectional study". *J. Healthc. Eng*, article ID 4071645, 2021.

[12] R. C. Lyle, "A performance test for assessment of upper limb function in physical rehabilitation treatment and research", Int. J. Ther Rehabil, vol. 4, no. 4, pp. 483-492, 1981, doi: 10.1097/00004356-198112000-0000.

[13] M. Dragovich, "Categorization and validation of handedness using latent class analysis," *Acta Neuropsychiatr*, vol. 16, no. 4, pp. 212–218, 2004.

[14] A. Schwarz, C. M. Kanzler, O. Lambercy, A. R. Luft, J. M. Veerbeek, "Systematic review on kinematic assessments of upper limb movements after stroke", *Stroke*, vol. 50, no. 3, pp. 718-727, 2019.

[15] A. Hussain *et al*., "Self- paced reaching after stroke: A quantitative assessment of longitudinal and directional sensitivity using the H-Man planar robot for upper limb neurorehabilitation". *Front Neurosci*, no. 10, 2016. DOI:10.3389/fnins.2016.00477.

[16] F. Marini *et al*., "Robotic wrist training after stroke: Adaptive modulation of assistance in pediatric rehabilitation". *Rob Auton Syst*, vol. 91, pp. 169-178, 2017. DOI: 10.1016/j.robot.2017.01.006.

[17] A. Arac. "Machine learning for 3D kinematic analysis of movements in neurorehabilitation", *Curr Neurol Neurosci Rep,* vol. 20, no. 8, pp. 29. DOI: 10.1007/s11910-020-01049-z.

[18] C. M. L. Hughes *et al*., "Developing an mHealth app for post-stroke upper limb rehabilitation: Feedback from U.S., and Ethiopian rehabilitation clinicians", *J Health Inform,* pp. 1-14. DOI: 10.1177/1460458219868356.